Research Square

Preprints are preliminary reports that have not undergone peer review.
They should not be considered conclusive, used to inform clinical practice,
or referenced by the media as validated information.

Microbe-Worm Symbiosis Stabilizes Methane Hydrates in Deep Marine Environments

Tianyi Hua
New York University https://orcid.org/0000-0002-8658-9594
Maisha Ahmad
New York University
Tenzin Choezin
New York University
Ryan Hartman (ryan.hartman@nyu.edu)
New York University https://orcid.org/0000-0002-5364-9933

Article

Keywords: Dynamic Stability, Microbial Bioreactions, Feather Duster Worms, Endothermic Methanogenic Metabolism, Methanotrophs

Posted Date: January 6th, 2021

DOI: https://doi.org/10.21203/rs.3.rs-125110/v1

License: This work is licensed under a Creative Commons Attribution 4.0 International License.
Read Full License

Version of Record: A version of this preprint was published at Energy & Fuels on November 22nd, 2021.
See the published version at https://doi.org/10.1021/acs.energyfuels.1c02673.

Microbe-Worm Symbiosis Stabilizes Methane Hydrates in Deep Marine Environments

*Tianyi Hua, Maisha T. Ahmad, Tenzin Choezin, and Ryan L. Hartman**

*Email: ryan.hartman@nyu.edu

Department of Chemical and Biomolecular Engineering, NYU Tandon School of Engineering, Brooklyn, New York, 11201, United States

Abstract

Our Planet has a natural ecosystem comprised of living organisms and methane hydrates in deep marine environments. This ecosystem was constructed in the present work to examine the influence that subtle temperature fluctuations could have on the dynamic stability of the hydrate deposits. The coupled mass and energy balance equations that describe the microbial bioreactions, their consumption by feather duster worms, and methane hydrate dissociation confirm that the bioreaction kinetics are dominated by endothermic methanogenic metabolism that stabilizes methane hydrates with a fragile tolerance to 0.001K temperature increases. The feather duster worms also stabilize the hydrates *via* their selective consumption of methanotrophs that could otherwise overtake the system by their exothermic metabolism. Critical ocean temperature limits exist, beyond which hydrate dissociations would cause underwater eruptions of methane into the sea. Historical ocean temperature records and gas hydrate inventory estimates combined with our model suggests that hydrate deposits as deep as 560-meters below sea level could already be at

risk, whereas the methane hydrate stability zone will retreat deeper as ocean temperatures rise. Slowing its retreat could avoid the massive release of greenhouse gas.

Introduction

Oceanic emissions contribute to natural atmospheric methane at a rate of 0.002 to 0.012 gigatons of methane per year.[1] Observations have suggested that a rise in the ocean temperature could induce the dissociation of the marine natural gas hydrates (comprised of >85% methane), and thereby release an enormous amount of methane into our atmosphere.[2–6] Natural gas hydrates are crystalline lattices of hydrogen-bonded water molecules that encapsulate small hydrocarbon (gas) molecules, such as methane[7]. Vital to sustain our planet, hydrates form spontaneously from water and small hydrophobic molecules under specific temperature and pressure conditions[8], such as in subsurface and suboceanic zones. With the vast quantity of methane (200 to 500 gigatons of CH_4) stored in marine hydrates world-wide[9], its sudden release due to rising ocean temperatures could cause catastrophic environmental impacts that are thought to have had historical significance in large mammal migratory patterns.[10]

In deep marine environments, methane is generated by one of two different processes: 'biogenic' methane as a product of methanogenic archaea metabolism, and 'thermogenic' methane from breaking down large organic molecules thermally near hot vents.[11] Isotopic studies of methane sources in natural settings have reported that biogenic methane are generally formed under a lower temperature and methanogenic microbes live near thermodynamic equilibrium.[12]

Methane hydrates located along continental margins have drawn increasing attention because that they are a modulator of climate change.[13]

In natural sedimentary environments, a variety of microbial communities coexist.[14–17] Methanotrophs are microbes that oxidize methane aerobically or anaerobically into biomass as their source of energy and carbon dioxide as metabolic waste. Methanogens, on the contrary, are microbes that produce methane as a product of their metabolic activity.[18] Anaerobic oxidation of methane (AOM), mediated by methane-oxidizing archaea, limits the flux of methane from marine environments to the atmosphere. Most methane in oceanic sediment is produced in organic rich areas by microbial methanogenesis.[14] Both carbon dioxide and acetate are believed to be important substrates for methanogenesis. Methanotrophy is generally exothermic, while methanogenesis is endothermic in general.[18] Although microbial metabolism kinetics are considerably slower than that of methane hydrate dissociation, any disruption in the energy balance could affect the stability of methane hydrates. Recently, Goffredi, S. K. *et al.* have discovered that feather duster worms (Sabellida, Annelida) have established a unique symbiosis with methanotrophic microbes.[19] In their study, worms engulfing methanotrophs as their energy source was captured by transmission electron microscopy. Methanotrophic microbes are a source of fuel for deep sea worm populations and extend the circle of carbon exchange in marine environments beyond microbial communities.

In the present work, we seek answers to the question of how stable methane hydrates are in their natural marine environment. The symbiotic ecosystem consisting of bacterial methanogens, methanotrophs, feather duster worms, and methane hydrates has fragile tolerance to ocean

temperature fluctuations that could destabilize our planet's natural methane hydrate ecosystem.[14,17–19]

Microbe-worm symbiosis with marine hydrates

Herein we considered the symbiosis shown in Figure 1 to demonstrate the equilibrium relationship between methane, methanogens, methanotrophs, and feather duster worms, outlining the carbon exchange routine in the system. As we now know, methane can be aerobically or anaerobically oxidized by methanotrophs into biomass and carbon dioxide. These methanotrophic microbes are constantly being consumed by deep-sea worms as their food resource. Substances produced by worms and from other sources can be reduced by methanogenic microbes back into methane. Under elevated pressure and reduced temperature in deep marine environments, methane forms methane hydrate with water.

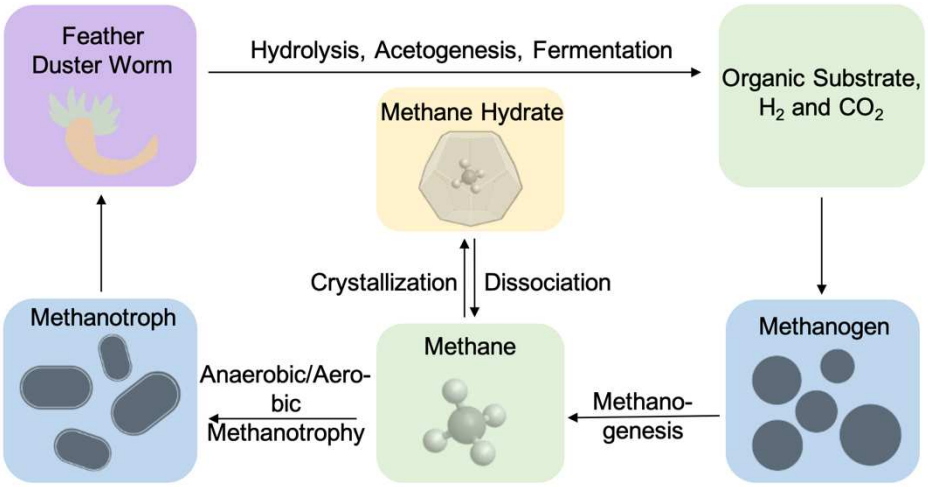

Figure 1. The symbiosis involving methanogens, methanotrophs, and feather duster worms, methane, and methane hydrates.

The microbial activities can be characterized as first order reactions with steady-state stoichiometry coefficients, whereas the filtration rate of the feather duster worm can be expressed as a suppression effect on methanotroph growth rate. By solving the differential equations

involving heat and mass balance of the symbiotic system, one can predict the concentration change of each species involved as well as the net heat exchange. Hence, one can estimate the stabilization effect on methane hydrates offered by the symbiotic system.

Marine natural gas hydrate inventory (GHI)

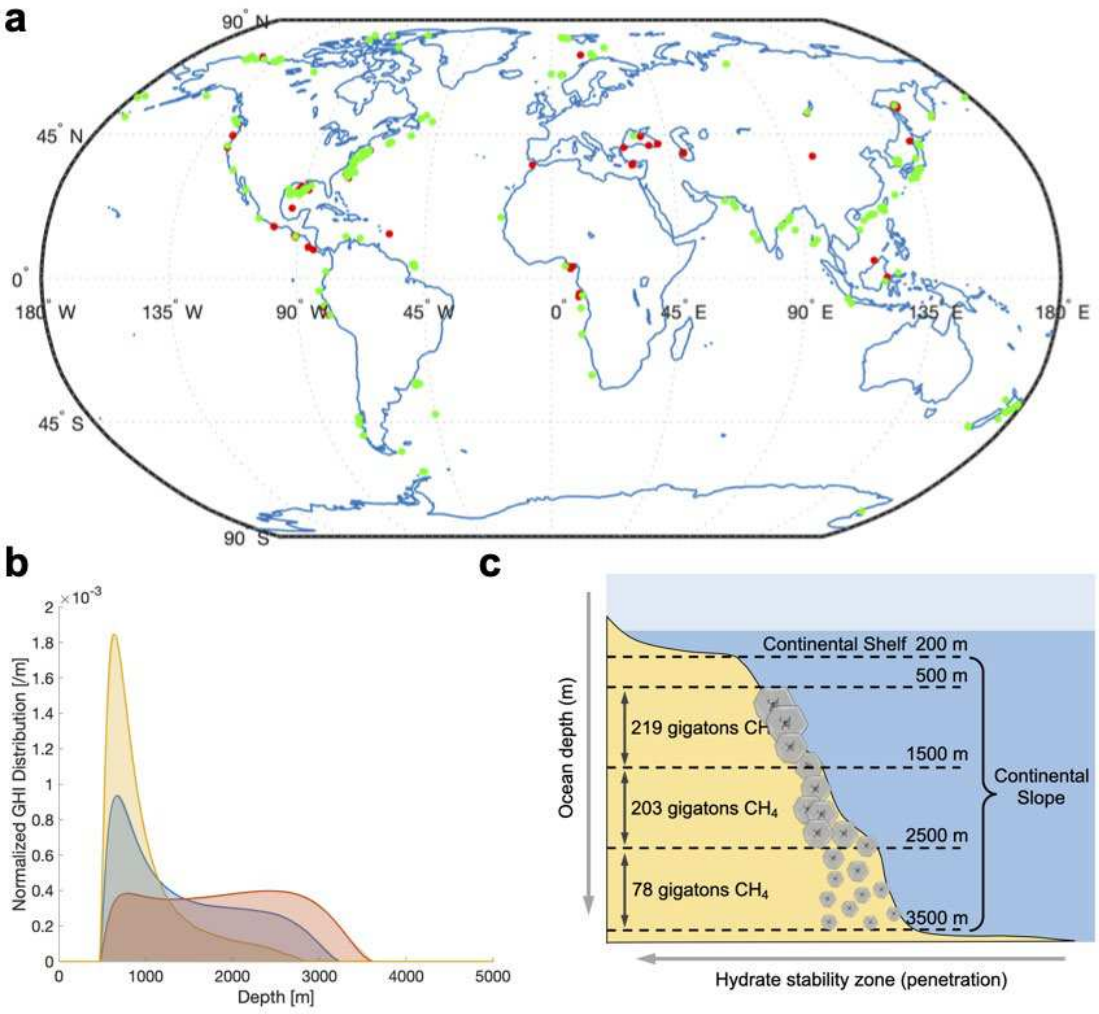

Figure 2. **a**, Known (**red**) and inferred (**green**) locations of gas hydrate. **b**, Normalized gas hydrate inventory (average value blue, with standard deviation yellow and red) distribution plotted against depth. **c**, Sketch of the methane hydrates deposited at different depths on the continental slope with estimated amount of methane carbon stored every 1000 m interval below 500 m. Methane hydrates invade sediments as the stability zone increases as depth increases.

The majority of the gas hydrates are deposited along the coast lines on the continental slope according to known and inferred gas hydrate locations data from *Waite et al.*[20], illustrated in Figure 2a. Using the model from *Kretschmer et al*[21], we are able to show in Figures 2b,c that the global gas hydrate inventory is mainly distributed between 500 m to 3500 m, where shallower distribution (500 to 1500 m) is limited by the lack of gas hydrate stability zone due to seawater temperatures above the hydrate phase boundary. The natural habitat of feather duster worms associated with methenotrophic symbionts overlaps with methane hydrate deposits, ranging from 300 m to 1800 m depth on record.[19] Seawater temperature decreases as depth increases, creating larger sub-cooling respect to methane hydrate phase boundary. Hence, deeper hydrates invade the marine sediments with a thicker gas hydrate stability zone. The deeper distribution (2500 to 3500 m) is limited by the insufficient sedimentation rate. It is within this thicker zone, at a greater depth, that one could expect confinement of the hydrates within nanopores of the minerology, which has been reported to depress their melting point.[22–24] In the other hand, hydrates deposited around 500 to 1500 m, also within the feather duster worm's habitat, are more sensitive to temperature fluctuations due to narrower stability zones, whereas deep gas hydrate deposits are more stable but only available at regions with high sedimentation. Our calculation also shows that approximately 43.8% (219 gigatons) of the total gas hydrate inventory (500 gigatons) are deposited at the shallower part of the continental slope (<1500 m) and 0.157% (0.0784 gigatons) are deposited at

a depth where seawater temperature is close to phase boundary (<600 m), vulnerable to potential temperature fluctuations.

Near-equilibrium energy balance simulations

Knowing the natural enviroment where methane hydrates could dissociate, we can calculate their dissociation kinetics based on the established mass and heat balances around the forementioned ecosystem. To estimate the rate of methane formation or consumption, we solved the constructured equations near the methane hydrate phase boundary, realistic of the scenario where the ocean temperature gradually increases. The presence of salts in seawater acts as a thermodynamic inhibitor, depressing the dissociation temperature of methane hydrate by a small amount compared to the freshwater system.[25] Phase boundaries of methane hydrates in fresh water and sea water are plotted using published data[13] in Figure S1, to account for the dissociation

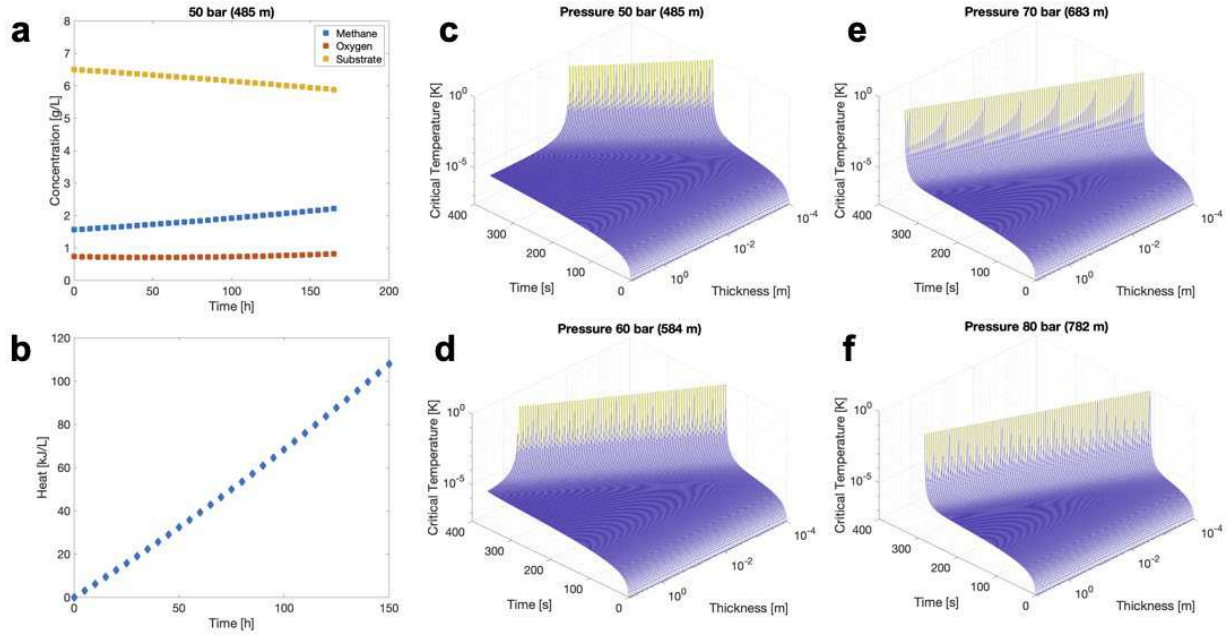

Figure 3. **a**, The concentration change of methane, oxygen, and substrate over time. **b**,The heat consumption over time. The critical temperature under different pressure (with the corresponding ocean depth) plotted against time and initial thickness of methane hydrate: **c**, 50 bar (485 m). **d**, 60 bar (584 m). **e**, 70 bar (683 m). **f**, 80 bar (782 m).

temperature depression in sea water. At a depth of 485 m, the corresponding pressure of 50 bar and temperature of 278.4 K yield Figure 3a. The result shows that under the given set of conditions, the methanogenesis reaction is predominate and heat is cumsumed over time. In other words, due to the difference between in metabolic activity and population density of methanogens and methanotrophs, there would be a net increase in methane concentration in their natural settings. Similarly, there would be a net decrease in the substrate concentration, and a net decrease in the oxygen concentration. It is important to note that the net heat is also negative, making the overall bioreaction endothermic. To further address the influence of the endothermic process on methane hydrates, we coupled the dissociation kinetics with the endothermic bioreaction. Based on previous research[26], methane hydrate dissocation can be de-coupled into two parts, intrinsic dissociation and heat transfer limited dissociation. The heat change can be written as:

$$\frac{dq_t}{dt} = \frac{dx}{dt} \cdot A\rho_H \Delta H_d = A\sqrt{\frac{\kappa \rho_H \Delta H_d \Delta T}{2t}} \quad (1)$$

And

$$\frac{dq_i}{dt} = k_d exp(-k_d t) V \rho_H \Delta H_d \quad (2)$$

Thus, the net heat change from methane dissocaition is written as:

$$\frac{1}{(\frac{dq}{dt})} = \frac{1}{(\frac{dq_t}{dt})} + \frac{1}{(\frac{dq_i}{dt})} \quad (3)$$

where, q_t and q_i are heat from heat treansfer and intrinsic methane dissociation, respectively, A is cross-section area, κ is thermal conductivity of methane hydrate, ρ_H is the density of methane hydrate, ΔH_d is the enthalpy of methane hydrate dissociation, ΔT is the temperature difference

between system and equilibrium, k_d is intrinsic methane hydrate dissociation rate constant, and V is the volume of bulk methane hydrate.

For a gradual increase in the ocean temperature, the heat change rate due to dissocation and the bioreaction are equilibrated near the phase boundary, and the result of which yields a critical temperature. This critical temperature is a function of initial methane hydrate thickness, pressure, and time. The results are plotted in Figure 3c-f. We can clearly see that at the beginning, the dissocation is dominated by intrinsic dissociation, and there is a sharp increase in the critical temperature for approximately tens of seconds. However, soon thereafter the dissociation becomes dominated by heat transfer, and thus the critical temperature reaches a plateau. Depending on the initial thickness of the methane hydrate, heat is transferred throughout the bulk methane hydrate over time, and finally its dissociation becomes dominated once again by intrinsic dissociation leading to a drastic increase in the critical temperature. Obviously, the width of the plateau is a function of the initial bulk methane hydrate thickness as the diffusive heat is a function of the material's thickness. Pressure, and hence ocean depth, as well contributes to the shape of the plateau as the phase boundary of methane hydrate shifts as pressure increases. At the final stage, microbial heat change is no longer comparable with methane hydrate dissociation heat change, causing a drastic increase in the critical temperature. Consequently, a catastrophic dissocation of the entire methane hydrate bulk would occur. It is important to note that the equilibrium between the bioreaction and methane hydrate dissociation is also influenced by biosurfactants secreted by microbes and those naturally dissolved in sea water.[27,28] Their predicted influence on the critical

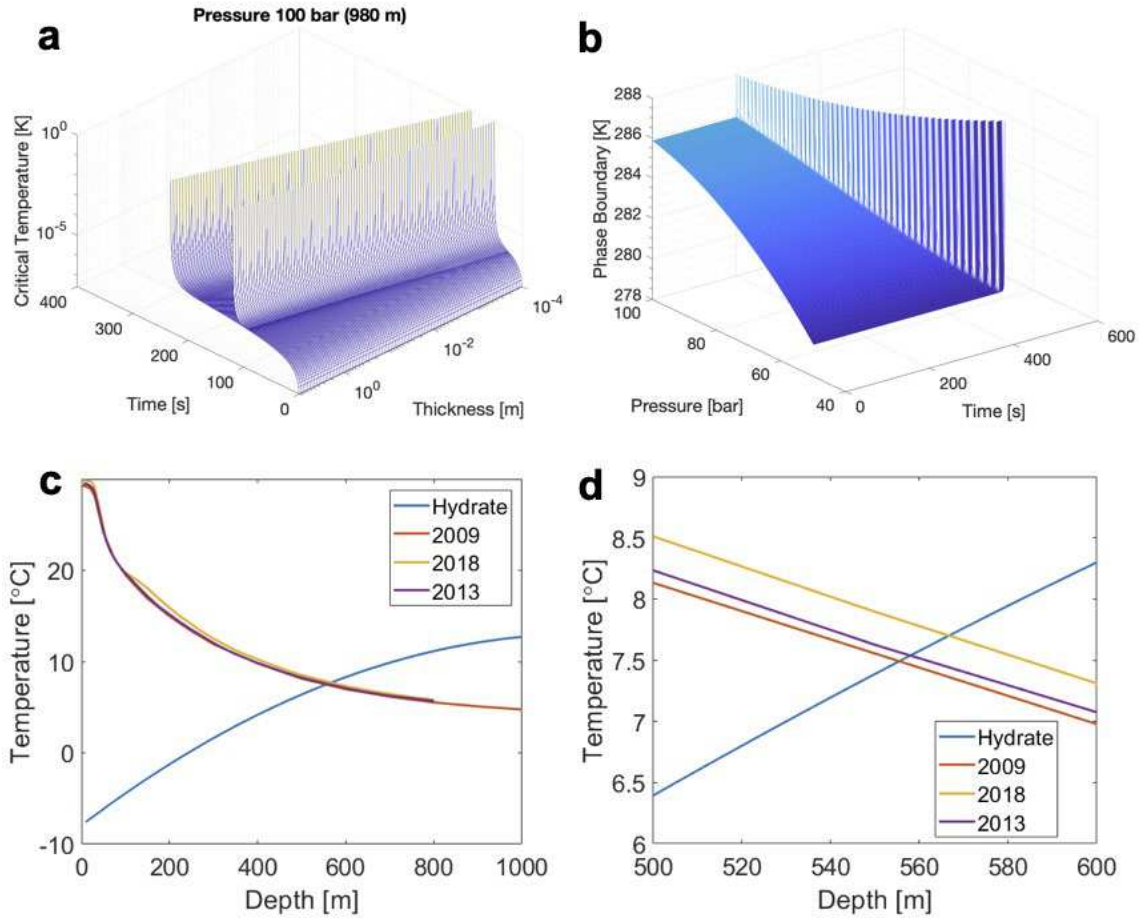

Figure 4. **a**, The width of critical temperature surface is influenced by biosurfactants secreted by microbes and those naturally occurring in sea water. **b**, Dynamic phase boundary of methane hydrate, with initial thickness of 8.7 m based on methane hydrate stability zone thickness, plotted against pressure (386 to 980 m) and time. **c**, Average summer sea water temperature in the Gulf of Mexico region at various depths plotted with the methane hydrate phase boundary in sea water. **d**, An expanded data set.

temperature was plotted in Figure 4a assuming a mixture of biosurfactant in sea water, with results at other pressures plotted as Figure S2 in Supplementary Infomation.

The methane hydrate phase boundary becomes dynamic in the presence of microbial activity and feather duster worms, and the recalculated phase boundary is plotted in Figure 4b. In the initial 400 s, the phase boundary of methane hydrate does not change much as the critical temperature is negligible compared to the phase boundary. However, after 400 s the phase

boundary runs into a 'wall', which is the point at which heat cannot be removed by conduction fast enough from the hydrate deposits, and thus catastrophic dissociation would occur. These findings support that a buffered zone of only hundreds of seconds wide is provided by the bioreaction of methanogenic and methanotrophic microbes. This fragile stabilization of critical temperature of 0.001 K would provide at best a weak isolation for methane hydrate dissociation due to environmental fluctuations.

To further evaluate the influence a change in the sea water temperature would have on methane hydrate stability, we collected data from the World Ocean Database[29–31] and the U.S. National Oceanic and Atmospheric Administration (NOAA)[32] to plot Figure 4c,d. As an example, the average sea water in the Gulf of Mexico region has increased consistently in the last decade where hydrates exist. The sea water temperature trajectory intercepts the methane hydrate phase boundary at a depth of 560 m, meaning that the natural methane hydrate deposits in this depth range are at risk due to the continuous increase in the temperature. Near-seafloor gas hydrates often contain hydrocarbons from methane through pentanes.[33] The phase boundaries of natural gas hydrates with typical composition[34,35] (~80% methane, ~10% ethane, ~4% propane, and others) were plotted in comparison with that of methane hydrates (Figure S3). The difference in phase equilibrium indicates that natural gas hydrates could stabilize at relatively shallower depths with repect to pure methane hydrates but have comparable sensitivity (T-P slope) to temperature fluctuations. At the depth of interest, the sea water temperature has inceased by half a degree from 2009 to 2018. This increase overshadows the critical temperature predictions of our calculations. Our findings support that if the temperature continues to rise, then despite of the stabilization effect from microbial activity, marine methane hydrates could face catastrophic dissociation. Our results motivate that actions are needed to slow down the retreat of the gas hydrate stability zone due to

rising ocean temperatures, to avoid a massive release of greenhouse gas by catastrophic dissociations of marine natural gas hydrates in continental margins.

Implications on the release of methane from marine deposits

Disruption of our planet's natural ecosystem could have significance on the release of methane from deep marine environments. Our results indicate that a microbe-feather duster worm symbiosis does stabilize the methane hydrates. Simulations of the equilibrium confirm that ocean temperature fluctuations could destabilize such a sensitive ecosystem; throwing it into a scenario of catastrophic underwater eruption. Herein we solved the coupled mass and energy balance equations that describe the microbial bioreactions, their consumption by feather duster worms, and methane hydrate dissociation, demonstrating that the bioreaction kinetics are dominated by methanogenic metabolism that stabilizes methane hydrates with a fragile tolerance to 0.001 K temperature increases. Our findings indeed support that critical ocean temperature limits exist, beyond which the catastrophic release of methane would be irreversible due to a heat transfer limited dissociation mechanism. Historical ocean temperature records combined with our model suggest that methane hydrate deposits as deep as 560-meters below sea level could already be at risk, whereas the methane hydrate stability zone would retreat deeper at a rate of 60-meters per degree temperature rise. Global predictions of natural gas hydrate distribution support that the majority of the marine gas hydrates are located in the coastal region on the continental slope, undergirding our concern that shallow gas hydrates are vulnerable to temperature fluctuations.

The implications of this work further suggest that even if the ocean temperature ceases to rise at depths greater than 560-meters hydrates could still dissociate. Based on our findings, an imbalance in the feather duster worm population could adversely influence the hydrates' stability. Decreases in worm population could weaken the suppression on methanotroph growth rate, in

which scenario the overgrowth of methanotroph would generate excess amount of heat and destabilize the hydrates. Similarly, a change in the microbial activity could impact the hydrates. An increase in methanogenic microbial activity would make the system more endothermic, thus strengthen the tolerance to temperature fluctuations close to methane hydrate phase boundary. Whereas an increase in methanotrophic activity would have the opposite effect.

Once the methane is released into the ocean, it is expected to recrystallize into hydrates as the water temperature and pressure in close proximity to the deposits would favor the hydrate formation region. One could expect a phenomenon of underwater snowing, whereby recrystallized hydrates rise in the water column, due to their lower in density than the surrounding sea water. The concentration of hydrates at shallower depths increases overtime as a product of successive warming and cooling, dissociation and crystallization.[36] Eventually, the crystals would dissociate to release the methane as the ocean temperature increases and the pressure decreases. Methane released at the sea floor by a catastrophic eruption may also be retained by a number of mechanisms. It could recrystallize on geological formations, on suspended particles by heterogeneous nucleation, or by a water-hydrate core-shell mechanism and eventually deposited elsewhere. Molecular dynamic simulations showed the possibility of forming methane nanobubbles suspended in seawater supersaturated with methane from hydrate dissociation.[37] Ocean currents may also result the deposition of the free-flowing hydrate crystals. These discoveries motivate that actions are needed to slow down the retreat of the gas hydrate stability zone due to rising ocean temperatures, to avoid a potential massive release of greenhouse gas by catastrophic dissociations of marine natural gas hydrates.

Methods

Mass and energy balances with the combined bioreaction kinetics were constructed based on the ecosystem described in Figure 1. Methanotrophy and methanogenesis can be expressed by the following bioreactions as[38]:

$$\text{Methanothrophy: } CH_4 + 1.45O_2 \rightarrow 0.52S + 0.48CO_2 \quad (4)$$

$$\text{Methanogenesis: } S \rightarrow CH_4 \quad (5)$$

where the chemistry is described by steady-state stoichiometric coefficients.

As a result, the rate of methane concentration change and bioreaction heat exchange can be described using Monod-like kinetics[38–40]:

$$\frac{dM}{dt} = phi\frac{0.92\mu_{gen}S}{K_s + S + S^2/K_i} - \mu_{troph}\frac{M}{K_M + M}\frac{O}{K_O + O} \quad (6)$$

$$phi = \exp\left(\frac{-6900}{R}\frac{1}{T} - \frac{1}{298}\right) \quad (7)$$

$$\frac{dH_{bio}}{dt} = 0.52\mu_{troph}\frac{M}{K_M + M}\frac{O}{K_O + O}\Delta H_{troph} + phi\frac{0.92\mu_{gen}S}{K_s + S + S^2/K_i}\Delta H_{gen} \quad (8)$$

$$\frac{d\mu_{troph}}{dt} = -k_{worm} \quad (9)$$

where, M is concentration of methane, O is oxygen concentration, S is the organic substrate concentration, μ_{gen} and μ_{troph} are the specific maximun growth rates of methanogenesis and methanotrophy, respectively, K_M, K_S, and K_i are Monod-like kinetic constants, H_{bio} is the overall heat change of the bioreactions, ΔH_{gen} and ΔH_{troph} are the enthalpy of methanogenesis and methanotrophy, respectively, and k_{worm} is the filteration rate of methanotrophs by feather duster worms. All the kinetic contants were adopted from published data as listed in Supplementary Infomation to fit in our calculation.[14,19,41] The rate of concentration change of oxygen and organic

substrate can be calculated using the stoichiometry of expressions (4) and (5). By solving the coupled mass and energy balance equations, with respect to boundary conditions of natural settings, we are able to caculate the methane comsumption over time and the occumulative heat comsumption. The MATLAB codes used to solve the system of equations are provided in the Supplementary Infomation.

To estimate how much methane hydrate could be affected by the rising sea temperatures, we calculated the gas hydrate inventory, GHI, as a function of depth below sea-level, z, using a model proposed by *Kretschmer et al*[21] :

$$GHI = a \cdot L_{GHSZ}^{b}(z) \cdot (POC_0 - \frac{c}{w(z)^d}) \cdot \exp\left(-(e + f \cdot \ln(w(z)))^2\right) \quad (10)$$

where, the following fitting parameters are used: $a = 0.002848 \pm 0.00049$, $b = 1.681 \pm 0.027$, $c = 24.42 \pm 7.2$, $d = 0.9944 \pm 0.10$, $e = -1.441 \pm 0.19$, and $f = 0.3925 \pm 0.032$. Here, L_{GHSZ} is gas hydrate stability zone thickness within marine sediment, which can be calculated by solving the steady state geotherm:

$$L_{GHSZ} = \frac{\kappa_B (T_m(z) - T_{bw}(z))}{q_H} \quad (11)$$

where $\kappa_B = 1.5\ W/m/K$, $q_H = 63\ mW/m^2$, and T_m and T_{bw} are the temperature of methane hydrate boundary and bottom seawater temperature, respectively. Sedimentation rate, w, is also a function of depth, z, which can be epressed as:

$$w = \frac{w_1}{1 + \left(\frac{z}{z_1}\right)^{c_1}} + \frac{w_2}{1 + \left(\frac{z}{z_2}\right)^{c_2}} \quad (12)$$

with $w_1 = 0.117\ cm/yr$, $w_2 = 0.006\ cm/yr$, $z_1 = 200\ m$, $z_2 = 4000\ m$, $c_1 = 3$, and $c_2 = 10$.

The global distribution of particulate organic carbon (POC_0) in marine surface sediments are based on the statistical data from *Seiter et al*[42] with 95% confidence. The MATLAB codes used here can also be found in Supplementary Infomation.

Acknowledgment

This material is based upon work supported by the Materials Research Science and Engineering Center (MRSEC) program of the National Science Foundation under Award Number DMR-1420073. Any opinions, findings, and conclusions or recommendations expressed in this material are those of the authors and do not necessarily reflect the views of the National Science Foundation.

Author Contributions

The manuscript was written through contributions of all authors. Conceptualization: R.L.H.; Data curation: T.H. and M.A.; Formal analysis: T.H., M.A., and T.C.; Funding acquisition: R.L.H.; Investigation: T.H., M.A., and T.C.; Methodology: T.H. and R.H.; Project administration: R.L.H.; Resources: R.L.H.; Software: T.H.; Supervision: R.L.H.; Validation: T.H.; Visualization: T.H. and M.A.; Writing – original draft: T.H.; Writing – review & editing: T.H. and R.L.H. Corresponding: R.L.H. All authors have given approval to the final version of the manuscript.

Competing Interests Statement

There are no conflicts of interest to declare.

References

1. Weber, T., Wiseman, N. A. & Kock, A. Global ocean methane emissions dominated by shallow coastal waters. *Nat. Commun.* **10**, 4584 (2019).

2. Reagan, M. T. & Moridis, G. J. Large-scale simulation of methane hydrate dissociation

along the West Spitsbergen Margin. *Geophys. Res. Lett.* **36**, L23612 (2009).

3. Westbrook, G. K. *et al.* Escape of methane gas from the seabed along the West Spitsbergen continental margin. *Geophys. Res. Lett.* **36**, L15608 (2009).

4. Maslin, M., Owen, M., Day, S. & Long, D. Linking continental-slope failures and climate change: Testing the clathrate gun hypothesis. *Geology* **32**, 53 (2004).

5. Kennett, J. P., Cannariato, K. G., Hendy, I. L. & Behl, R. J. *Methane Hydrates in Quaternary Climate Change: The Clathrate Gun Hypothesis*. pp. 105-105 (American Geophysical Union, 2003).

6. de Garidel-Thoron, T., Beaufort, L., Bassinot, F. & Henry, P. Evidence for large methane releases to the atmosphere from deep-sea gas-hydrate dissociation during the last glacial episode. *Proc. Natl. Acad. Sci.* **101**, 9187–9192 (2004).

7. Sloan, E. D. Fundamental principles and applications of natural gas hydrates. *Nature* **426**, 353–359 (2003).

8. Koh, C. A. Towards a fundamental understanding of natural gas hydrates. *Chem. Soc. Rev.* **31**, 157–167 (2002).

9. Milkov, A. V. Global estimates of hydrate-bound gas in marine sediments: how much is really out there? *Earth-Science Rev.* **66**, 183–197 (2004).

10. Lister, A. M. & Stuart, A. J. The impact of climate change on large mammal distribution and extinction: Evidence from the last glacial/interglacial transition. *Comptes Rendus Geosci.* **340**, 615–620 (2008).

11. Wuebbles, D. Atmospheric methane and global change. *Earth-Science Rev.* **57**, 177–210

(2002).

12. Stolper, D. A. *et al.* Distinguishing and understanding thermogenic and biogenic sources of methane using multiply substituted isotopologues. *Geochim. Cosmochim. Acta* **161**, 219–247 (2015).

13. Dickens, G. R. & Quinby-Hunt, M. S. Methane hydrate stability in seawater. *Geophys. Res. Lett.* **21**, 2115–2118 (1994).

14. Sivan, O., Schrag, D. P. & Murray, R. W. Rates of methanogenesis and methanotrophy in deep-sea sediments. *Geobiology* **5**, 141–151 (2007).

15. Billard, E., Domaizon, I., Tissot, N., Arnaud, F. & Lyautey, E. Multi-scale phylogenetic heterogeneity of archaea, bacteria, methanogens and methanotrophs in lake sediments. *Hydrobiologia* **751**, 159–173 (2015).

16. Buriánková, I. *et al.* Methanogens and methanotrophs distribution in the hyporheic sediments of a small lowland stream. *Fundam. Appl. Limnol. / Arch. für Hydrobiol.* **181**, 87–102 (2012).

17. Yoshioka, H. *et al.* Activities and distribution of methanogenic and methane-oxidizing microbes in marine sediments from the Cascadia Margin. *Geobiology* **8**, 223–233 (2010).

18. Evans, P. N. *et al.* An evolving view of methane metabolism in the Archaea. *Nat. Rev. Microbiol.* **17**, 219–232 (2019).

19. Goffredi, S. K. *et al.* Methanotrophic bacterial symbionts fuel dense populations of deep-sea feather duster worms (Sabellida, Annelida) and extend the spatial influence of methane seepage. *Sci. Adv.* **6**, eaay8562 (2020).

20. Waite, W.F., Ruppel, C.D., Boze, L-G., Lorenson, T.D., Buczkowski, B.J., McMullen, K.Y., and Kvenvolden, K. A. Preliminary global database of known and inferred gas hydrate locations: U.S. Geological Survey data release. *U.S. Geol. Surv.* (2020).

21. Kretschmer, K., Biastoch, A., Rüpke, L. & Burwicz, E. Modeling the fate of methane hydrates under global warming. *Global Biogeochem. Cycles* **29**, 610–625 (2015).

22. Casco, M. E. *et al.* Methane hydrate formation in confined nanospace can surpass nature. *Nat. Commun.* **6**, 6432 (2015).

23. Uchida, T. *et al.* Decomposition of methane hydrates in sand, sandstone, clays, and glass beads. *J. Geophys. Res. Solid Earth* **109**, B05206 (2004).

24. Mekala, P., Babu, P., Sangwai, J. S. & Linga, P. Formation and Dissociation Kinetics of Methane Hydrates in Seawater and Silica Sand. *Energy & Fuels* **28**, 2708–2716 (2014).

25. Loh, M. *et al.* Dissociation of Fresh- And Seawater Hydrates along the Phase Boundaries between 2.3 and 17 MPa. *Energy & Fuels* **26**, 6240–6246 (2012).

26. Chen, W. & Hartman, R. L. Methane Hydrate Intrinsic Dissociation Kinetics Measured in a Microfluidic System by Means of in Situ Raman Spectroscopy. *Energy & Fuels* **32**, 11761–11771 (2018).

27. Bhattacharjee, G. *et al.* The Biosurfactant Surfactin as a Kinetic Promoter for Methane Hydrate Formation. *Energy Procedia* **105**, 5011–5017 (2017).

28. Arora, A. *et al.* Biosurfactant as a Promoter of Methane Hydrate Formation: Thermodynamic and Kinetic Studies. *Sci. Rep.* **6**, 20893 (2016).

29. Locarnini, R. A., A. V. Mishonov, J. I. Antonov, T. P. Boyer, H. E. Garcia, O. K. Baranova,

M. M. Zweng, and D. R. J. *World Ocean Atlas 2009*. (NOAA Atlas NESDIS 68, U.S. Government Printing Office, 2010).

30. Boyer, T.P., J. I. Antonov, O. K. Baranova, C. Coleman, H. E. Garcia, A. Grodsky, D. R. Johnson, R. A. Locarnini, A. V. Mishonov, T.D. O'Brien, C.R. Paver, J.R. Reagan, D. Seidov, I. V. Smolyar, and M. M. Z. *World Ocean Database 2013*. (NOAA Atlas NESDIS 72, 2013).

31. Boyer, T.P., O. K. Baranova, C. Coleman, H. E. Garcia, A. Grodsky, R. A. Locarnini, A. V. Mishonov, T.D. O'Brien, C.R. Paver, J.R. Reagan, D. Seidov, I. V. Smolyar, K. Weathers, and M. M. Z. *World Ocean Database 2018 (Pre-release)*. (2018).

32. Boyer, Tim P.; Biddle, Mathew; Hamilton, Melanie; Mishonov, Alexey V.; Paver, Christopher R.; Seidov, Dan; Zweng, M. M. *Gulf of Mexico Regional Climatology (NCEI Accession 0123320)*. (NOAA National Centers for Environmental Information, 2015).

33. Milkov, A. V. Molecular and stable isotope compositions of natural gas hydrates: A revised global dataset and basic interpretations in the context of geological settings. *Org. Geochem.* **36**, 681–702 (2005).

34. Topham, D. R. The formation of gas hydrates on bubbles of hydrocarbon gases rising in seawater. *Chem. Eng. Sci.* **39**, 821–828 (1984).

35. Saberi, A., Alamdari, A., Shariati, A. & Mohammadi, A. H. Experimental measurement and thermodynamic modeling of equilibrium condition for natural gas hydrate in MEG aqueous solution. *Fluid Phase Equilib.* **459**, 110–118 (2018).

36. Thatcher, K. E., Westbrook, G. K., Sarkar, S. & Minshull, T. A. Methane release from

warming-induced hydrate dissociation in the West Svalbard continental margin: Timing, rates, and geological controls. *J. Geophys. Res. Solid Earth* **118**, 22–38 (2013).

37. Bagherzadeh, S. A., Alavi, S., Ripmeester, J. A. & Englezos, P. Evolution of methane during gas hydrate dissociation. *Fluid Phase Equilib.* **358**, 114–120 (2013).

38. Petersen, L. A. H. *et al.* Dynamic investigation and modeling of the nitrogen cometabolism in Methylococcus capsulatus (Bath). *Biotechnol. Bioeng.* **116**, 2884–2895 (2019).

39. Villadsen, J., Nielsen, J. & Lidén, G. *Bioreaction Engineering Principles*. 3rd Ed., p. 561 (Springer US, 2011).

40. Yang, S. T. & Okos, M. R. Kinetic study and mathematical modeling of methanogenesis of acetate using pure cultures of methanogens. *Biotechnol. Bioeng.* **30**, 661–667 (1987).

41. Tamaru, C. S. *et al.* Growth and Survival of Juvenile Feather Duster Worms, Sabellastarte spectabilis, Fed Live and Preserved Algae. *J. World Aquac. Soc.* **42**, 12–23 (2011).

42. Seiter, K., Hensen, C., Schröter, J. & Zabel, M. Organic carbon content in surface sediments—defining regional provinces. *Deep Sea Res. Part I Oceanogr. Res. Pap.* **51**, 2001–2026 (2004).

Figure Legends

Figure 1. The symbiosis involving methanogen, methanotroph, and feather duster worms, methane, and methane hydrates.

Figure 2. **a**, Known (**red**) and inferred (**green**) locations of gas hydrate. **b**, Normalized gas hydrate inventory (average value blue, with standard deviation yellow and red) distribution plotted against

depth. **c**, Sketch of the methane hydrates deposited at different depths on the continental slope with estimated amount of methane carbon stored every 1000 m interval below 500 m. Methane hydrates invade sediments as the stability zone increases as depth increases.

Figure 3. **a**, The concentration change of methane, oxygen, and substrate over time. **b**,The heat consumption over time. The critical temperature under different pressure (with the corresponding ocean depth) plotted against time and initial thickness of methane hydrate: **c**, 50 bar (485 m). **d**, 60 bar (584 m). **e**, 70 bar (683 m). **f**, 80 bar (782 m).

Figure 4. **a**, The width of critical temperature surface is influenced by biosurfactants secreted by microbes and those naturally occurring in sea water. **b**, Dynamic phase boundary of methane hydrate, with initial thickness of 8.7 m based on methane hydrate stability zone thickness, plotted against pressure (386 to 980 m) and time. **c**, Average summer sea water temperature in the Gulf of Mexico region at various depths plotted with the methane hydrate phase boundary in sea water. **d**, An expanded data set.

Figures

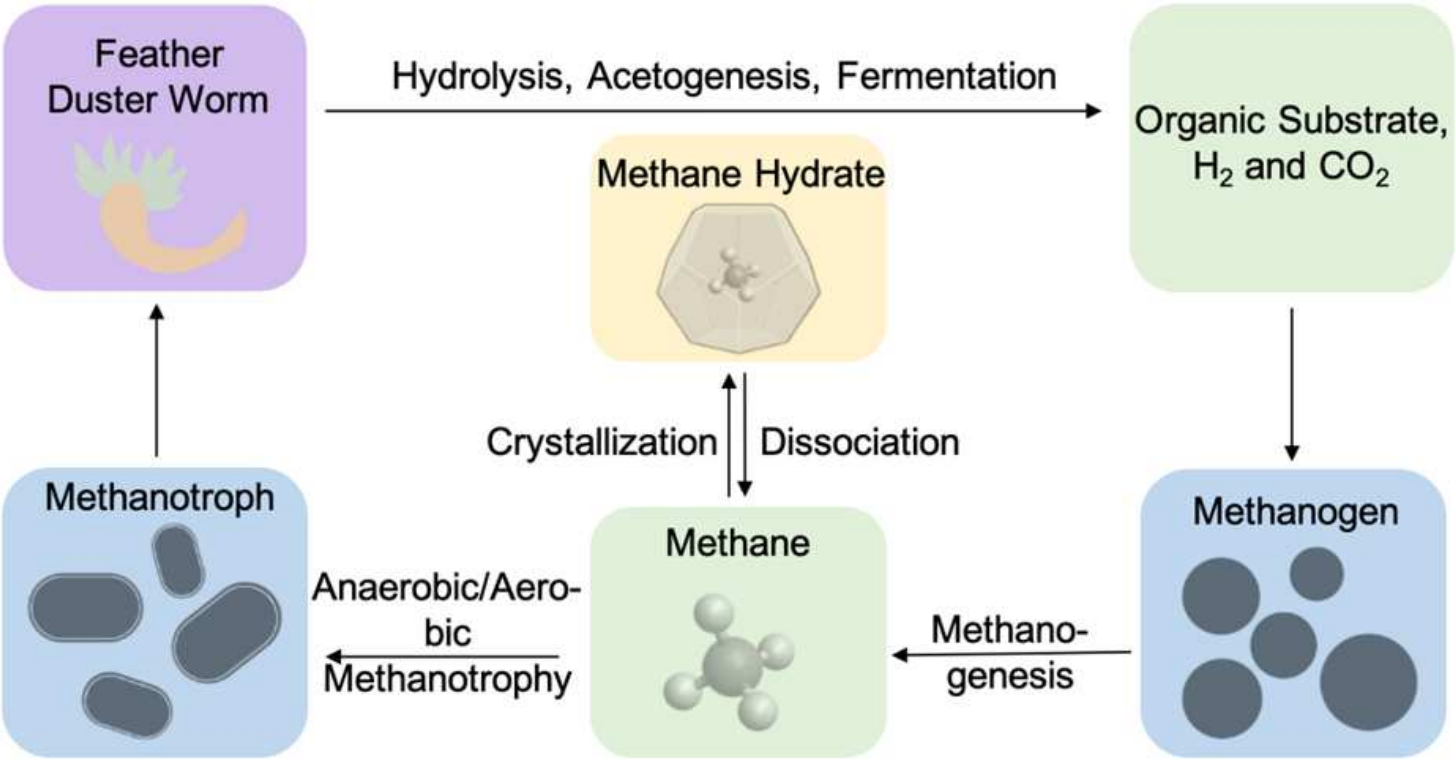

Figure 1

The symbiosis involving methanogens, methanotrophs, and feather duster worms, methane, and methane hydrates.

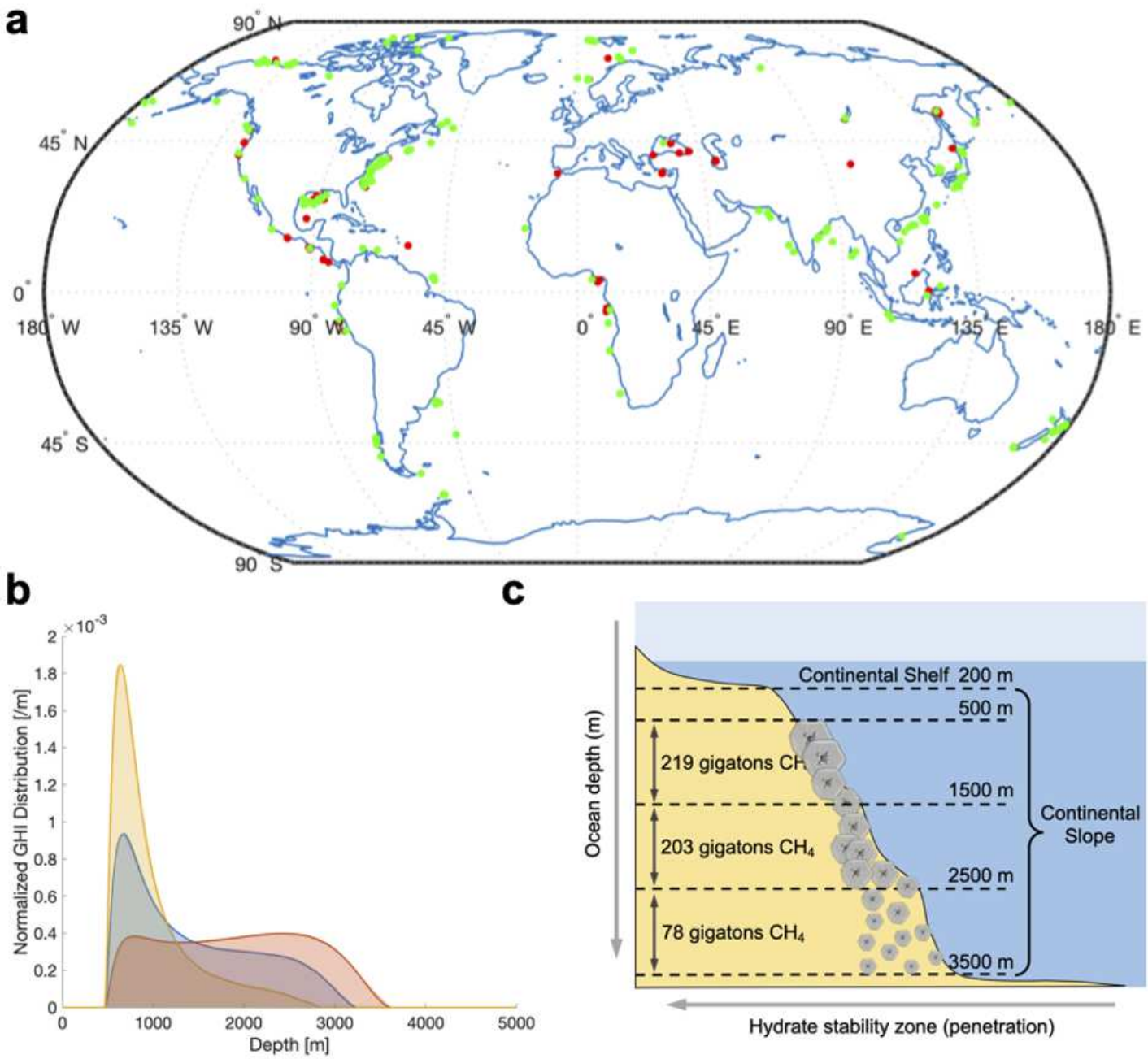

Figure 2

a, Known (red) and inferred (green) locations of gas hydrate. b, Normalized gas hydrate inventory (average value blue, with standard deviation yellow and red) distribution plotted against depth. c, Sketch of the methane hydrates deposited at different depths on the continental slope with estimated amount of methane carbon stored every 1000 m interval below 500 m. Methane hydrates invade sediments as the stability zone increases as depth increases.

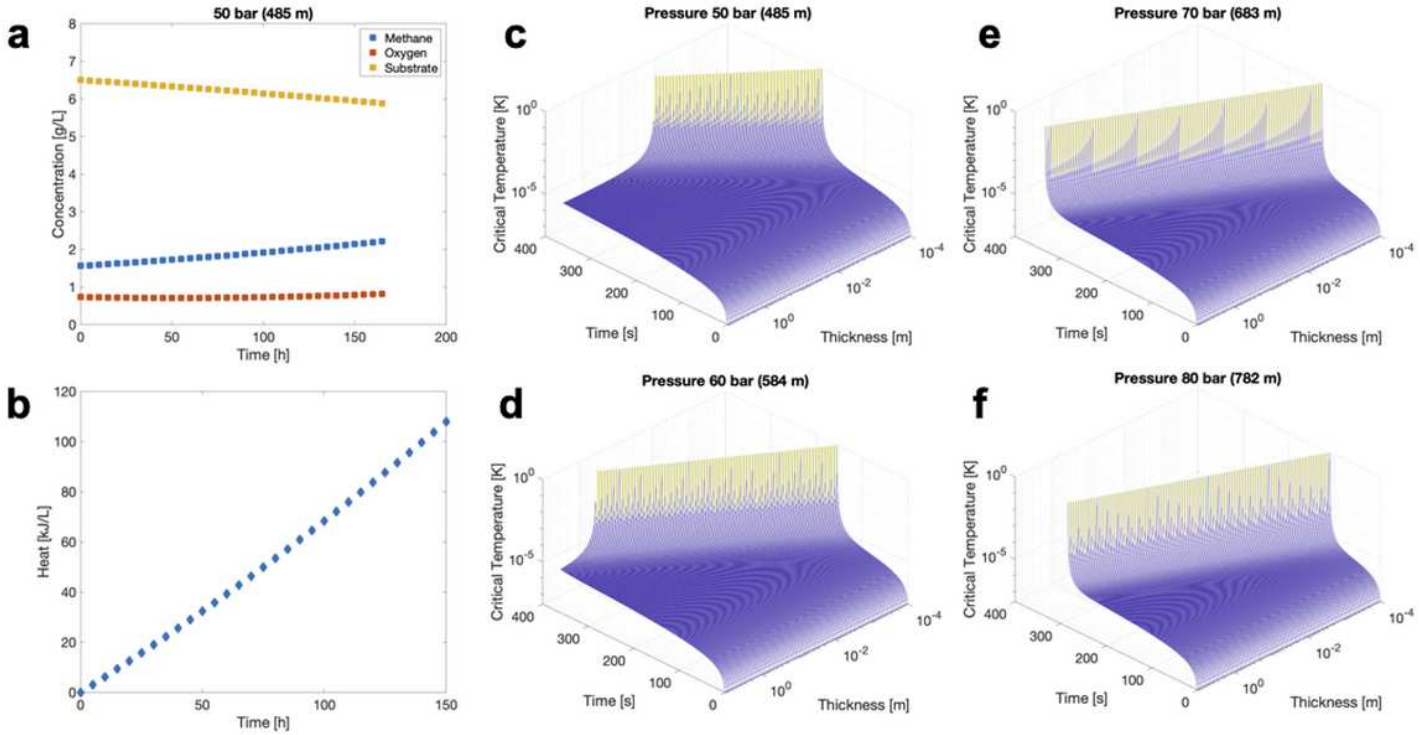

Figure 3

a, The concentration change of methane, oxygen, and substrate over time. b,The heat consumption over time. The critical temperature under different pressure (with the corresponding ocean depth) plotted against time and initial thickness of methane hydrate: c, 50 bar (485 m). d, 60 bar (584 m). e, 70 bar (683 m). f, 80 bar (782 m).

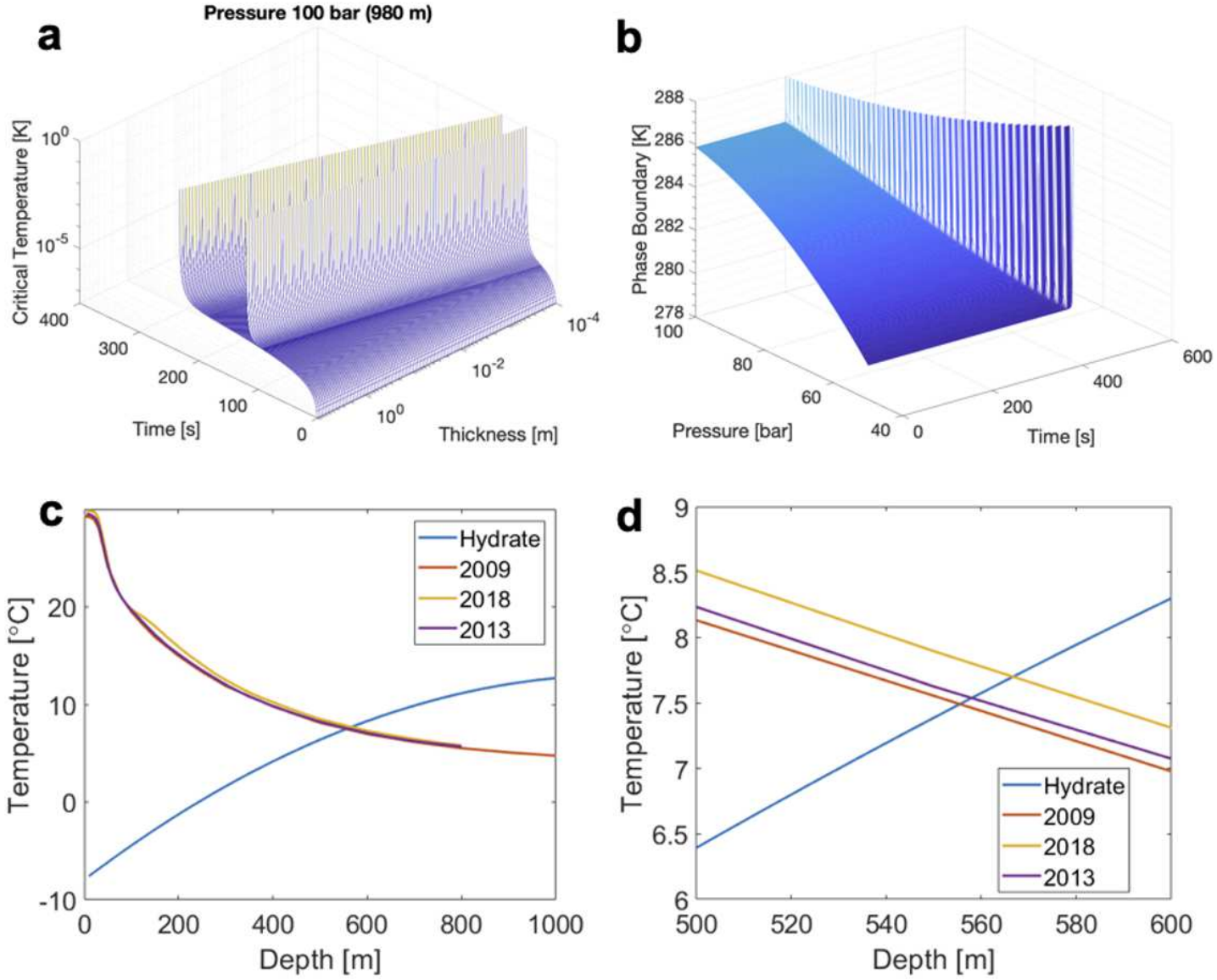

Figure 4

a, The width of critical temperature surface is influenced by biosurfactants secreted by microbes and those naturally occurring in sea water. b, Dynamic phase boundary of methane hydrate, with initial thickness of 8.7 m based on methane hydrate stability zone thickness, plotted against pressure (386 to 980 m) and time. c, Average summer sea water temperature in the Gulf of Mexico region at various depths plotted with the methane hydrate phase boundary in sea water. d, An expanded data set.

Supplementary Files

This is a list of supplementary files associated with this preprint. Click to download.

- Supplementaryinformation.pdf